Sulfur evolution of the 1991 Pinatubo magmas based on apatite

Ashley E. Van Hoose [a],*, Martin J. Streck [a], John S. Pallister [b], Markus Wälle [c]

[a] Department of Geology, Portland State University, 17 Cramer Hall, 1721 SW Broadway, Portland, OR 97207, USA
[b] U.S. Geological Survey, David A. Johnston Cascades Volcano Observatory, 1300 SE Cardinal Court, Building 10, Suite 100, Vancouver, WA 98683-9589, USA
[c] Institut für Geochemie und Petrologie, Departement Erdwissenschaften, ETH Zurich, Clausiusstr. 25, 8092 Zurich, Switzerland

ARTICLE INFO

ABSTRACT

Using electron microprobe (EMP) and laser-ablation inductively coupled plasma mass spectrometry (LA-ICP-MS) to collect major and rare-earth elements (REE), respectively, from apatites from the 1991 Mt. Pinatubo juvenile eruption products, we have determined that two statistically distinct populations of apatite exist. One population crystallized from the juvenile basaltic melt (*basalt* apatites) and the other population crystallized from the main dacitic magma body (*silicic* apatites). Both populations contain high-S apatites (>0.7 wt.% SO_3). Apatite has previously been shown to be a potential monitor for magmatic sulfur contents via numerous proposed coupled substitutions of P^{5+} for S^{6+}. However, simple apatite/melt partitioning cannot account for high-S silicic apatites, which grew from a silicic melt with an apparent maximum S concentration of ~80 ppm. Disparate apatite morphology (i.e. skeletal and acicular for basalt apatites and euhedral for silicic apatites) as well as compositional evidence reveal that high-S silicic apatites were not inherited from the juvenile basalt during mingling/mixing prior to eruption. Sulfur gain from neighboring anhydrite phenocrysts can also be ruled-out as a source of high sulfur. EMP sulfur mapping of silicic apatites shows highly irregular patterns of sulfur enrichment that do not correspond with adjacent anhydrite and can be found within apatites hosted by other minerals (e.g. hornblende and Fe–Ti oxides). With these data in mind, we propose high-S silicic apatites from Pinatubo and other sulfur-rich systems achieved elevated sulfur concentrations during high sulfur fluxing events that originated from underplated basalt during degassing of a SO_2-rich fluid phase. That basalts were indeed sulfur rich and oxidized is here indicated by high S contents of apatites growing in basalt. The predominant location of S-rich areas of silicic apatite is crystal interiors of apatite inclusions in other mineral phases, while large apatite microphenocrysts surrounded by groundmass glass have low sulfur contents. This is evidence for placing sulfur-fluxing periods long before events that ultimately led to the 1991 eruption.

© 2013 Elsevier B.V. All rights reserved.

1. Introduction

The 1991 eruptions of Mount Pinatubo (Pinatubo), Philippines, ended a 500 year hiatus in activity (Newhall et al., 1996) and were triggered by basaltic recharge into the 50 km³ dacitic magma reservoir (Pallister et al., 1992, 1996), releasing 20 million tons of SO_2 into the stratosphere (Bluth et al., 1992; Daag et al., 1996). Three distinct juvenile magmatic components were erupted over the course of the eruption. Dacite pumices of two varieties erupted during the June 15th climactic eruption including 1) a white, phenocryst-rich dacitic pumice (~85 vol.%), and 2) a tan, phenocryst-poor dacitic pumice (~15 vol.%). Prior to that, a hybrid-andesite lava containing quenched basaltic inclusions erupted between June 7th and 12th forming a lava dome (Bernard et al., 1996; David et al., 1996; Pallister et al., 1996).

The objective of this study is to constrain the conditions of the formation of high-sulfur apatites in silicic magmas using the well-documented 1991 Pinatubo system as a framework and to test the following hypothetical sulfur sources: 1) mafic magmas from which high-S apatites could be inherited; 2) neighboring anhydrite phenocrysts, which could generate high-S apatite through diffusion; or 3) a separate, SO_2-rich fluid phase from which high-S apatite and anhydrite could have crystallized. We will explore each of these scenarios; eliminate the first two, and confirm the third. We also offer a hypothesis about the mechanism by which the S-enrichment in apatite took place.

We found that S-bearing apatites occur in all three juvenile components, yet observed S content is variable. Basaltic magma includes only high-S (>0.7 wt.% SO_3) apatites, while dacitic and hybrid andesite magmas carry low- (<0.3 wt.% SO_3), medium- ($0.3-0.7$ wt.% SO_3), and high-S apatites. Our results indicate that: 1) basaltic high-S apatite crystallized rapidly as the basalt was quenched during mingling/mixing and that these apatite grains are not chemically related to the high-S apatites of silicic magmas; 2) S-diffusion from anhydrite phenocrysts to *silicic* high-S apatite did not occur and likely cannot occur; and 3) punctuated, high flux of a SO_2-rich fluid from underplating

* Corresponding author at: School of the Environment, Washington State University, 1228 Webster Phys. Sciences Bldg., 100 Dairy Road, Pullman, WA 99164-1120, USA. Tel.: +1 360 600 1994 (cell); fax: +1 509 335 3700.
E-mail addresses: ashley.vanhoose@wsu.edu (A.E. Van Hoose), streckm@pdx.edu (M.J. Streck), jpallist@usgs.gov (J.S. Pallister), waelle@erdw.ethz.ch (M. Wälle).

basaltic magma is the most probable process by which *silicic* high-S apatite is grown in the Pinatubo and similar systems.

2. Samples and methods

2.1. Samples

Samples for this study were obtained from the collection at the Cascades Volcano Observatory (CVO) USGS in Vancouver, WA. The samples are representative of three of the four juvenile magmatic components from the 1991 Pinatubo eruption and were collected shortly after the climactic eruption. The samples are: phenocryst-rich dacitic pumice, PH12C (64 wt.% SiO_2) collected from the Bucao drainage on the northwest flank of Pinatubo, hybrid andesite lava, CN6791-d (59 wt.% SiO_2), and a basalt inclusion, P-22892-2a (51 wt.% SiO_2). Both the andesite and basalt samples were collected from the Maraunot River drainage northwest of the current caldera. The phenocryst-poor dacitic pumice was not included in this study due to a lack of sufficiently sized and preserved crystals. The two pumice types exhibit identical mineralogies and chemical compositions, including both major and trace elements. It has been suggested that the difference in types is strictly due to a change from a sudden and violent eruptive episode early in the climactic June 15 eruption, to a less violent, more sustained eruption (David et al., 1996). The violent nature in the early eruption physically shattered any crystals that had grown in the magma reservoir, as evidenced in the abundant and small (<10 μm to <1 μm) crystal fragments observed in the phenocryst-poor type (Bernard et al., 1996; David et al., 1996; Pallister et al., 1996).

2.2. Electron microprobe (EMP) analysis

Apatites and melt inclusions from thin sections were analyzed for major elements using a five-spectrometer CAMECA SX 100 electron microprobe at Oregon State University. Analyses were performed via remote access at Portland State University. Analytical conditions for apatite analyses were as follows: 15 keV accelerating voltage, 20 nA beam current, and 2 μm beam diameter. Peak acquisition times were as follows: Na, P, Mn, and Ca 10 s; Mg, Fe, and Cl 20 s; Si and F 30 s; and S and Ce 60 s. Background acquisition times were half of the peak acquisition times for all analyses. The main purpose of these EMP analyses was to determine the sulfur content and intra-grain variability across apatite grains using traverse analyses (Fig. 1). Melt inclusions (in plagioclase and hornblende phenocrysts) and matrix glass were analyzed with a 10 μm beam diameter and a beam current of 8 nA. A large beam diameter and low currents were used to minimize beam damage and consequent alkali element migration. Peak acquisition times were: Na (counted first), Al, Si, K, and Fe 10 s; F, P, Ti, Mn, and Ca 20 s; Mg and Cl 30 s; and S 40 s. In order to reduce the detection limit for S to ~50 ppm, we reanalyzed glasses during a second round of analyses using a beam current of 30 nA and peak acquisition time for S of 120 s. Background counts were half those of peak times in all circumstances. Natural minerals were used as standards including: Durango fluorapatite (FLAP; USNM 104021), anhydrite (ANHY), and tugtupite (TUGT). Care was taken to analyze the same FLAP crystal for each EMP session to decrease the effects of crystallographic orientation on halogen concentrations (Stormer et al., 1993; Pyle et al., 2002; see Appendix A).

Additionally, several of the apatites with a high S domain were selected for element mapping of S, Na, F, Cl, and P to produce a more complete picture of sulfur distribution within a given grain. Most of these grains were smaller apatites that were unsuitable for LA-ICP-MS (i.e. the grains had diameters smaller than the minimum laser diameter, 15 μm). Apatites selected for element mapping were hosted within primarily anhydrite, but also hornblende and Fe–Ti oxides. Apatite element mapping operating conditions were an accelerating voltage of 15 keV, a beam current of 30 nA, and a point dwell time of 40 ms.
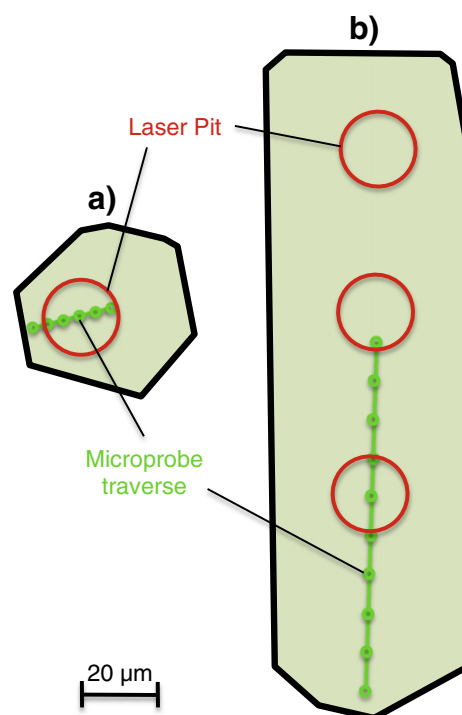

Fig. 1. Illustration of the method used to correlate major element data collected with EMP (traverse) and trace element data collected with LA-ICP-MS (large circles). Laser spots were selected to overlap the microprobe traverse. Major element values used with trace element data are the average of the EMP spots overlapped by the laser spot. Two examples of apatites: a) apatite cut perpendicular to the c-axis with a single laser spot; b) apatite cut parallel to the c-axis with multiple laser spots.

2.3. Laser-ablation inductively coupled plasma mass spectrometry (LA-ICP-MS)

Trace element data, including REE, were acquired on apatites, anhydrites, plagioclase, hornblendes, and glass on thick sections using LA-ICP-MS analyses. Data were acquired using the 193 nm ArF Excimer Laser coupled with an ELAN 6100 ICP quadrupole mass spectrometer at Eidgenössische Technische Hochschule (ETH) Zürich, Switzerland. Laser settings were 23, 24, 28, and 30 kV and a 10 Hz repetition rate, yielding a fluence of about 12 J/cm^2 on the ablation site. For apatites, beam sizes of 15, 20, and 40 μm were used. To ensure data consistency, a large crystal of Durango apatite was also analyzed. These analyses agree well with published values (Table 1), generally within 10% for most trace elements (Kimura et al., 2000; Marks et al., 2012).

Apatites selected for LA-ICP-MS analyses had to be large enough for the sizeable laser spots. Dacite-, andesite-, and basalt-hosted apatites were selected with a variable range of SO_3 including low (<0.3 wt.%), medium (0.3–0.7 wt.%), and high (>0.7 wt.%) as determined by prior microprobe data. Locations of EMP traverses were recorded on petrographic microscope images taken of the apatites. Using these images, laser spot positions were selected to overlap the pre-existing EMP traverses (Fig. 1). Some apatites were large enough for up to four laser spots, but the majority of crystals were large enough for only one spot. Host minerals were also analyzed using 15, 20, and 40 μm beam sizes appropriate for individual crystals. Compositions of host minerals were used to identify contamination of the apatite analysis in cases where the laser beam size was close to the size of the apatite.

The MATLAB-based program, SILLS, was used to process all LA-ICP-MS data (Guillong et al., 2008). SILLS requires both an internal and external standard to quantify element concentrations. NIST 610 was the external standard used at ETH, and the internal standard